https://doi.org/10.1016/j.jre.2020.07.020

Enhancing de/hydrogenation kinetics properties of the Mg/MgH_2 system by adding ANi_5 (A = Ce, Nd, Pr, Sm, and Y) alloys via ball milling

Wenfang Liao[a], Wenbin Jiang[a], Xu-Sheng Yang[c, d, *], Hui Wang[a], Liuzhang Ouyang[a, b, *], Min Zhu[a, b]

[a]School of Materials Science and Engineering, Guangdong Provincial Key Laboratory of Advanced Energy Storage Materials, South China University of Technology, Guangzhou, 510641, People's Republic of China. E-mail: meouyang@scut.edu.cn

[b]China-Australia Joint Laboratory for Energy & Environmental Materials, Key Laboratory of Fuel Cell Technology of Guangdong Province, Guangzhou, 510641, People's Republic of China

[c]Advanced Manufacturing Technology Research Centre, Department of Industrial and Systems Engineering, The Hong Kong Polytechnic University, Hung Hom, Kowloon, Hong Kong, China. Email: xsyang@polyu.edu.hk

[d]Hong Kong Polytechnic University Shenzhen Research Institute, Shenzhen 518057, China

Abstract

Magnesium (Mg)-based alloys have already been widely studied as the hydrogen storage materials because of their high reversible hydrogen storage capacity, low cost, and light weight, etc. However, the poor de/hydrogenation kinetic properties dramatically hinder the practical applications. In this work, the MgH_2–ANi_5 (A = Ce, Nd, Pr, Sm, and Y) composites have been prepared by a high-energy ball milling, which can effectively refine the particle size thus improving the kinetic properties. Experimental results reveal that the MgH_2–ANi_5 composites mainly consist of Mg_2NiH_4, MgH_2 and Rare earth (RE) hydride, which will be dehydrogenated to form Mg_2Ni, Mg and stable RE hydride reversibly. Accordingly, the as-milled MgH_2–ANi_5 (A = Ce, Nd, Pr, Sm, and Y) composites with various A-elements can respectively contribute a reversible hydrogen storage capacity of 6.16 wt%, 5.7 wt%, 6.21 wt%, 6.38 wt%, and 6.5 wt% at a temperature of 300 ˚C, and show much better kinetic properties in comparison with the pure MgH_2 without any additive. In-situ formed Mg_2Ni and stable RE hydride (such as $CeH_{2.73}$ and YH_2) might act as effective catalysts to significantly improve the hydrogen storage properties of MgH_2. The present work provides a guideline on improving the kinetic properties of the Mg-based hydrogen storage alloys.

Keywords: Mg-based hydrogen storage alloy; kinetic properties; ANi_5; Additives;

1. Introduction

Hydrogen is one of the most promising clean energy resources because of its high energy density, environmental friendliness, and renewability.[1] However, there is a huge challenge to store and transport hydrogen. Apart from the hydrogen storage in gaseous and liquid states, solid-state hydrogen storage has been considered as the most reliable safe and practical solution.[2-4] In particular, Magnesium (Mg)-based alloys are considered one of the most promising solid-state hydrogen storage materials due to their high hydrogen storage capacity (e.g., 7.6 wt% in the case of MgH_2), abundance, low cost and light weight.[5] Nevertheless, the high thermodynamic stabilities (ΔH = 75 kJ/mol), sluggish kinetics (Ea = 156 kJ/mol) and poor reversible cycling properties greatly hinder their practical applications.[6, 7] For example, the catalyst-free MgH_2 starts to desorb hydrogen at a temperature as high as 350 ˚C with rather slow kinetics due to the existence of a surface oxide layer[8] and the quite small H diffusion coefficient between Mg and MgH_2.[7, 9]

In order to overcome these drawbacks, numerous efforts have been made to enhance the hydrogen storage performance of MgH_2, such as the addition of catalysts to enhance the kinetic properties,[10, 11] the combination of metal or metal hydride to improve the thermodynamic stabilities,[12, 13] and the reduction of particle size, etc. Particularly, additives or catalysts have been explored extensively because of their striking effects in improving the hydrogen storage performance of MgH_2.[14, 15] Accordingly, combining MgH_2 with additives or catalysts such as metal,[16] hydrides,[17, 18] metal halides,[19, 20] metal oxides,[11, 21, 22] carbon-based materials[23, 24] and nanosized alloys[25] have been explored. More specifically, adding some transition metals, which are located in Group IIIB-VB and Period 4-6 in the period table, can enhance the ability to form stable hydrides under relatively moderate temperature and pressure,[26-28] and also enhance hydrogen storage kinetic properties. For example, G. Liang, et al.[29] studied the effect of the addition of

$LaNi_5$ on the hydrogen storage properties of mechanically milled MgH_2/Mg, finding that the ternary Mg–Ni–La alloy has much better absorption and desorption kinetics than the binary Mg–La and Mg–Ni alloys. Pavel et al.[30] synthesized nanocomposites of MgH_2-transition metallic hydrides (ScH_2, YH_3, TiH_2, ZrH_2, VH, and NbH), demonstrating that these transition metallic hydrides can not only lead to the easier combination of hydrogen atoms during desorption but also form coherent interfaces between MgH_2 and transition metallic hydrides that favor the later nucleation. Ouyang et al.[31] prepared the $CeH_{2.73}$-MgH_2-Ni nanocomposites with in-situ formed stable $CeH_{2.73}$ which can catalyze the hydriding/dehydriding process by combining with Ni to Mg/MgH_2. Notably, this in-situ formed nanocomposites structure can effectively suppress Mg/MgH_2 grain growth and enable the material to maintain its high performance after more than 500 cycles. In addition, the primary-precipitated metal Mg phase on the surface of MgH_2 can act as nucleate precursors and $CeH_{2.73}$ remains stable during absorption/desorption process, serving as a hydrogen pump, which is similar to the dehydrogenation steps and factors controlling desorption kinetics of Mg-Ce hydrogen that was referred by Xie et al.[32] It has also been found that RE-based alloy co-doping Ce-Y fabricated by Yong et al.[33] can release hydrogen completely in 42 min at 340 ˚C, 100 min at 320 ˚C, 320 min at 300 ˚C, respectively. While Zhang et al.[34] reported that MgH_2-5 wt%Ni_3C composites can release the hydrogen of 6.3 wt%, 6.2 wt% and 3.3 wt% in 20 min at 325 ˚C, 300 ˚C, and 275 ˚C, respectively.

The above description indicates clearly that the addition of suitable catalysts, especially the transition RE-based metals or compounds, can effectively improve the kinetic performance of Mg-based hydrogen storage alloys. In this work, a series of transition and RE elements have been chosen to form the MgH_2-ANi_5 (A = Ce, Nd, Pr, Sm, and Y) nanocomposites by high-energy ball milling to improve the hydrogen storage kinetic properties of Mg-based alloy. The results show that as-milled nanocomposites exhibit a faster dehydrogenation rate and better kinetic properties in comparison with the pure Mg/MgH_2

system. The present work provides a helpful guideline on improving the kinetic properties of the Mg content-based hydrogen storage alloys.

2. Experimental details

2.1 Preparation of MgH_2–ANi_5 composites

The states of raw alloy materials are shown in the table 1. Commercial MgH_2 powders (20 μm, 98% purity) were directly used without any other processing and ANi_5 (A = Ce, Nd, Pr, Sm, and Y) pieces were melted by arc melting. MgH_2 (95 wt%) and ANi_5 (5 wt%) were weighed and manually mixed in desired weight fraction using a stainless-steel dipper which contributed to a uniform distribution of the composition. It is worth noting that the theoretical hydrogen storage capacity of the mixture is 7.2 wt%. The high-energy ball milling was employed to process the mixture including MgH_2 and different ANi_5 under the 2.5 MPa hydrogen atmosphere which was a mixture of 5% hydrogen and 95% argon. The ball milling process was conducted with a ball-to-powder mass ratio of 30:1, the rotational speed was 1200 r/min, and every 30 min milling followed by 30 min interval for rest. Note that all operations were performed in the glovebox under the protection of high purity argon atmosphere to prevent the oxidation of the samples.

Table 1

Information of raw materials.

Material	Purity	Form	Size /μm(mesh)
MgH_2	98.0%	Powder	≤20.0
$CeNi_5$	99.9%	Granule	≤187.5 (80)
$NdNi_5$	99.9%	Granule	≤187.5 (80)
$SmNi_5$	99.9%	Granule	≤187.5 (80)
YNi_5	99.9%	Granule	≤187.5 (80)
$PrNi_5$	`99.9%	Granule	≤187.5 (80)

2.2 Characterizations

The phase constitutes of the as-milled compounds were characterized by X-Ray diffraction (XRD,

DX-2700) which is equipped by a Philips X'Pert MPD X-ray diffractometer with Cu Kα radiation (λ = 0.154 nm). The morphologies, particle sizes and chemical compositions of the samples were examined by scanning electron microscope (SEM-Zeiss Supra 40/VP). Differential Scanning Calorimetry (DSC) measurements were conducted to investigate the desorption behavior by using a Netzsch Jupiter 449C equipment under argon flow from room temperature to 450 ˚C at a heating rate of 5 ˚C/min.

The hydrogen storage properties of all prepared samples were tested using a precise Sieverts-type apparatus Pro2000 equipped with the furnace for accurately controlling temperature within 2 ˚C. Specifically, the kinetic curves were measured at temperatures of 300 ˚C, 325 ˚C and 350 ˚C, respectively, under the hydrogen pressure of 2.5 MPa for the absorption processes while 0.1 MPa for the desorption processes. The thermodynamic properties at different temperatures were measured by pressure composition isotherms (P.C.I) using an Advanced Materials Corporation (AMC) gas reaction controller. The middle point of the measured P.C.I curve was taken as the plateau pressure to mathematically fit the enthalpy ΔH and entropy ΔS during the absorption and desorption processing based on the van't Hoff plot.

3. **Results and discussion**

3.1 Optimization of ball-milling time

Based on the previous work,[35] $CeNi_5$ and MgH_2 can be milled under a hydrogen atmosphere. It is worth noting that the ball-milling time is an important parameter to impact hydrogen storage performance.[36] On one hand, the composition of the sample will be not uniform if the milling time is not enough, which might make the milled sample not activated fully. On the other hand, too long-term milling process might aggravate the oxidation condition. Therefore, either deficient or excess ball-milling time will cause the loss of hydrogen storage capacity.[37, 38] In the present work, ball milling processes of MgH_2-$CeNi_5$ sample with different time (i.e., 4 h, 6 h and 8 h) were conducted first to optimize ball-milling

time based on the kinetic properties. Fig. 1(a) and (b) give respectively the absorption and desorption kinetic curves of the MgH_2-$CeNi_5$ sample with different ball-milling times at a temperature of 320 ˚C. The MgH_2-$CeNi_5$ samples with a ball-milling time of 6 h own the highest absorption capacity and the fastest hydrogen desorption rate, e.g., absorbing hydrogen capacity of 6.1 wt% within less than 350 s, which is higher than that of 5.8 wt% in 4 h-milled samples and 5.6 wt% in 8 h-milled samples. Similarly, the sample with a ball-milling time of 6 h also possesses the best desorption kinetic properties with the highest desorption capacity and the fastest hydrogen desorption rate in comparison with 4 h-milled and 8 h-milled samples, as shown in Fig. 1(b). The preliminary experimental results indicate that the ball-milling time of 6 h might be the optimum parameter, which will be adopted to process all ANi_5 (A = Ce, Nd, Pr, Sm, and Y) samples and their hydrogen storage properties have been investigated in the following sections.

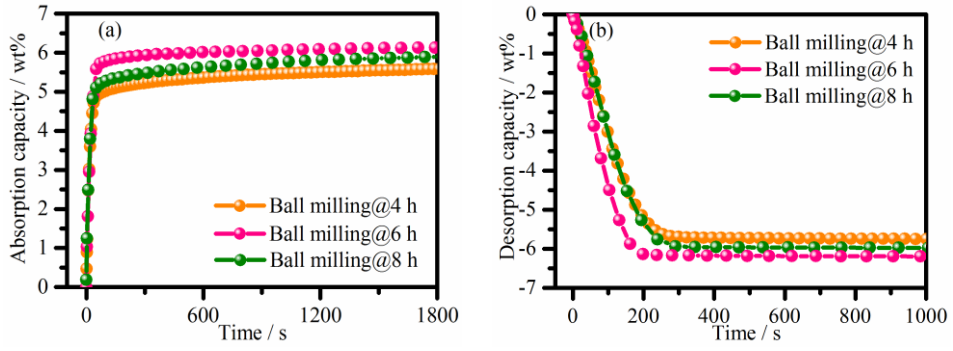

Fig. 1. Absorption (a) and desorption (b) kinetic curves of MgH_2-$CeNi_5$ with different ball-milling times at the temperature of 320 ˚C.

3.2 Phase transition during de/hydrogenation processes

Fig. 2 shows the XRD patterns of as-milled MgH_2-ANi_5 (A = Ce, Nd, Pr, Sm, and Y) composites, revealing that the milled composites possess multiphase structures, including the MgH_2 phase, Mg_2NiH_4 phase, AH_3 phase and some ANi_5 phase left. The hydrogenation pathways during the ball milling process can be therefore described as follows[39]

$$ANi_5 + 10MgH_2 \rightarrow 5Mg_2Ni + AH_{2.73} + 17.23H_2 \quad (1)$$

$$AH_{2.73} + 0.135H_2 \rightarrow AH_3 \quad (2)$$

$$Mg_2Ni + 2H_2 \rightarrow Mg_2NiH_4 \quad (3)$$

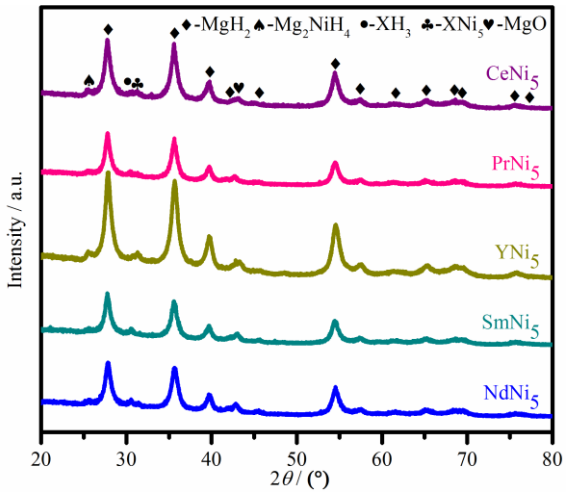

Fig. 2. The XRD patterns of as ball milled MgH_2-ANi_5 (A = Ce, Nd, Pr, Sm, and Y) composites.

Fig. 3(a) and (b) exhibit the SEM images of one of the initial melted YNi_5 alloys with the particle size ranging from 20-40 μm and the commercial MgH_2 powder with the particle size of 2-10 μm, respectively. After the ball milling process, the particle size of the obtained MgH_2-YNi_5 composites is refined, as the agglomerated particle composing of small granules ranging from nanoscale to 10 μm in the corresponding SEM image shown in Fig. 3(c). The milled composites with refined microstructure will induce numerous defects, which would act as the diffusion path of hydrogen and nucleation sites for the de-/hydrogenation processes. Besides, it's worth noting that hydrogen atoms existing in the lattice interstitial site of lattice during hydrogenation may cause high lattice stress and expansion. Nonetheless, the nanocrystalline and amorphous structures can be kept under this saturated hydrogenation state, meaning the excellent structural stability of the as-milled composites.

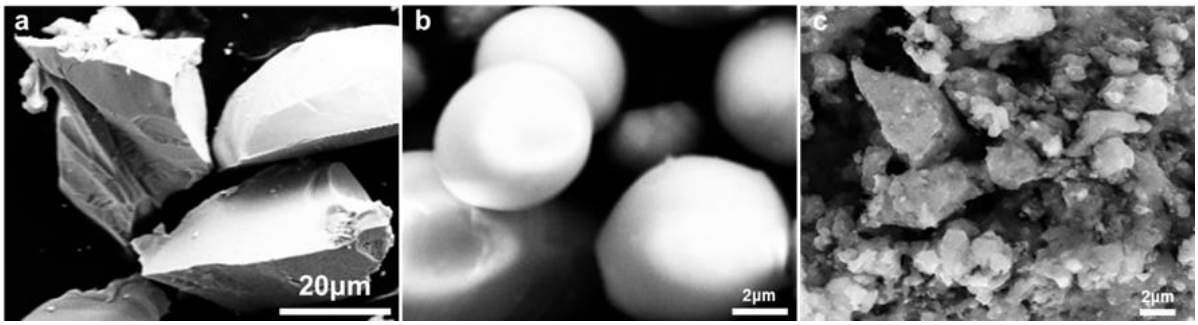

Fig. 3. The SEM images of (a) melted YNi_5 alloy (b) commercial MgH_2 powder and (c) as-milled MgH_2-YNi_5 composites.

To figure out the phase changes of the composites during hydrogenation and dehydrogenation processes, MgH_2-YNi_5 is selected as a representative, which will be characterized by XRD after fully hydrogenated and dehydrogenated as shown in Fig. 4. Combine with Fig. 2, XRD patterns of as-milled MgH_2-YNi_5 composite possess multiphase structures, including the phase of MgH_2, Mg_2NiH_4, YH_3, and some YNi_5 left. The XRD peaks become strong and sharp obviously after the hydrogenation cycles, which indicates that the particle sizes become bigger and the crystallinity is also increased. Besides, it can be seen that MgH_2 and Mg_2NiH_4 are dehydrogenated to form Mg and $Mg_2NiH_{0.3}$, respectively. Notably, RE hydrides YH_3 can only dehydrogenate partially to form stable phases such as YH_2 which always remain unchanged in the following whole de/hydrogenation processes.[40] As mentioned above, these stable phases serve as a hydrogen pump for controlling desorption kinetics of hydrogen storage alloys.[32] Besides, it is worth noting that a small amount of MgO phase is also detected in these alloys. The appearance of MgO is believed to be originated from some unavoidable testing process exposed to the air environment.

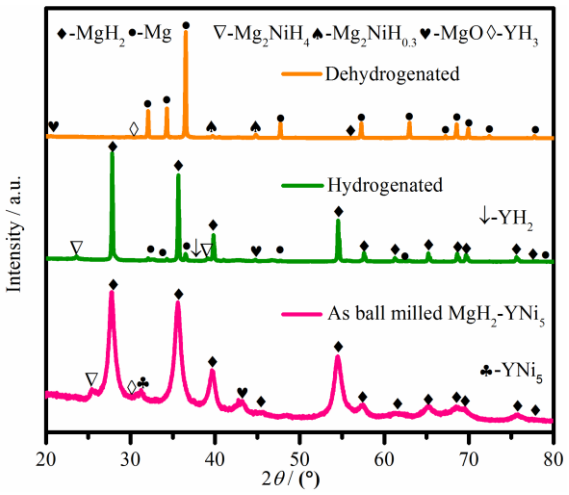

Fig. 4. The de/re-hydrogenation XRD pattern and its initial XRD pattern of MgH_2-YNi_5 composite.

3.3 Hydrogen absorption/desorption kinetics

The non-isothermal dehydrogenation performance of MgH_2-ANi_5 (A = Ce, Nd, Pr, Sm, and Y) alloys were investigated by DSC. The temperature-programmed desorption curve of saturated hydride alloys at a heating rate of 5 K/min is illustrated in Fig. 5. In each closed chamber, the mass of the sample is set equal to avoid the effect of desorption temperature from incremental pressure.

Compared with the dehydrogenation peak temperature of 423.4 ˚C of pure MgH_2 without any treatment, it is shown that those of as-milled MgH_2-ANi_5 (A = Ce, Nd, Pr, Sm, and Y) alloys are decreased to be 288.8 ˚C, 284.2 ˚C, 287.6 ˚C, 287.3 ˚C and 287.3 ˚C respectively. This suggests that the addition of ANi_5 alloys can effectively lower the desorption temperature of MgH_2, which might be ascribed to the weakened Mg-H bond caused by the electronic exchange reaction between RE elements and MgH_2.[41]

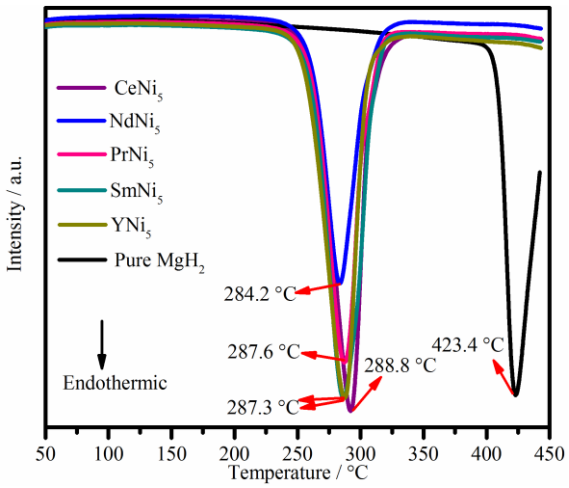

Fig. 5. The DSC curves of as-milled MgH_2-ANi_5 (A = Ce, Nd, Pr, Sm, and Y) alloys.

To inspect the influence of different ANi_5 alloys on kinetic properties of MgH_2, activation procedure was applied to the samples before conducting kinetics experiments. This procedure included several hydrogen absorption and desorption cycles which were done at 300 ˚C and under an initial 2.5 MPa for absorption and 0.1 MPa for desorption.

The absorption kinetic properties of as-milled MgH_2-ANi_5 composites were operated at 300 ˚C, 320 ˚C and 350 ˚C, respectively, under 2.5 MPa, as shown Fig. 6(a-c), where the absorption kinetic curve of pure MgH_2 processed by the same ball milling parameters is also provided for comparison. Notably, a rapid hydriding rate exhibits in all samples of achieving the almost saturated hydrogen absorption capacities within several minutes, after which there is nearly no increase in hydrogen absorption capacity. Specifically, five as-milled MgH_2-ANi_5 (A = Ce, Nd, Pr, Sm, and Y) composites samples can reach the saturated hydrogen capacities of 6.09 wt%, 6.07 wt%, 6.26 wt%, 6.1 wt% and 5.92 wt%, respectively, at the temperature of 300 ˚C within 9 min, showing the better absorption kinetic properties, compared with that of pure ball-milled MgH_2 which can reach a higher capacity after a quite long time. When the absorption temperatures are increased to 320 ˚C and 350 ˚C, however, it is found that the saturated hydrogen capacities and corresponding kinetics of five MgH_2-ANi_5 (A = Ce, Nd, Pr, Sm, and Y) composites are both worse than

those of pure ball-milled MgH_2. The experimental result in Fig. 6 indicates that the catalytic effect of ANi_5 alloys on MgH_2 particularly works at a relatively lower temperature level which will be also reflected in the following sections. These hydrogenation curve characteristics might be attributed to the mechanism that a surface-near hydride layer is formed within the initial few minutes so that the diffusion of hydrogen through this layer becomes a rate-limiting factor.[42]

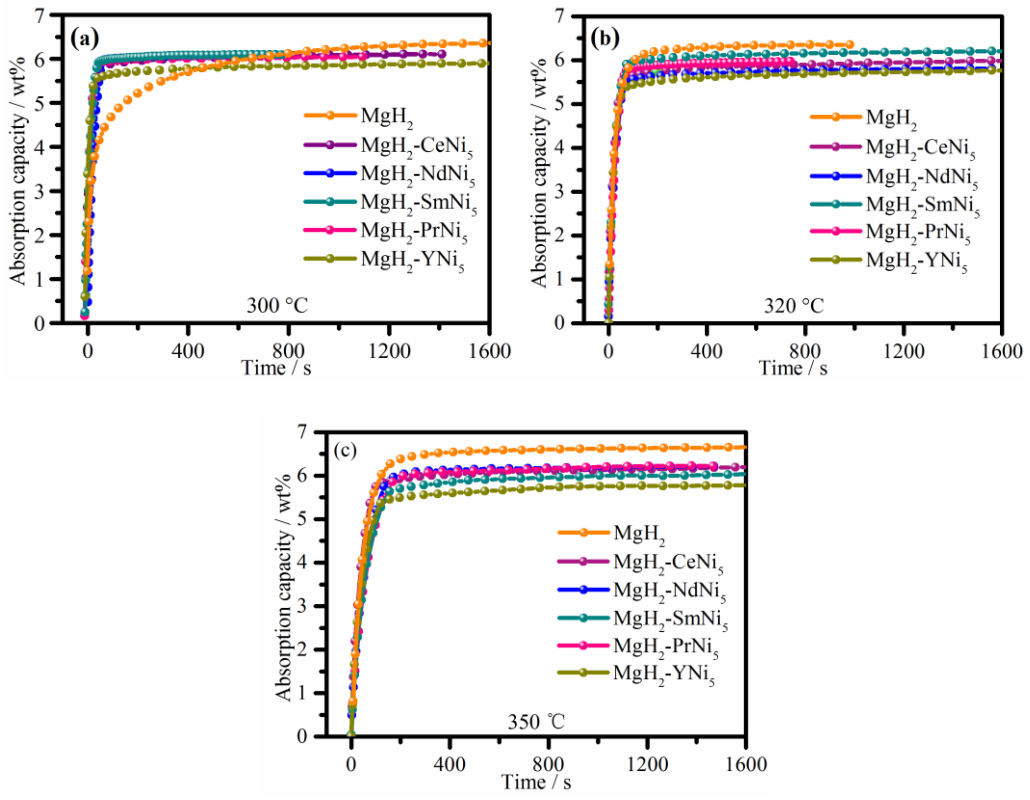

Fig. 6. The kinetic curves of hydrogen absorption of MgH_2-ANi_5 composites at different temperatures of (a) 300 ˚C, (b) 320 ˚C and (c) 350 ˚C respectively.

In addition to the hydrogenation kinetics, Fig. 7(a-c) gives the dehydrogenation kinetic curves of the as-milled MgH_2-ANi_5 composites samples at temperatures of 300 ˚C, 320 ˚C and 350 ˚C, respectively, under 0.1 MPa. Different from the hydrogenation kinetics, the addition of the ANi_5 leads to the dramatic improvement in dehydrogenation kinetics of MgH_2-ANi_5 composites for all temperature ranges, compared with that of pure milled MgH_2, as demonstrated clearly in Fig. 7(a-c). Note that the dehydrogenation

capacity of as-milled MgH_2-ANi_5 composites samples decreases slightly with temperature increasing.

The hydrogen storage properties and phase about all the ball-milled samples are summarized in table 2. Taking the experimental result at the temperature of 300 ˚C as an example, it is found that five as-milled MgH_2-ANi_5 (A = Ce, Nd, Pr, Sm, Y) can desorb hydrogen capacities of 6.16 wt%, 5.7 wt%, 6.21 wt%, 6.38 wt% and 6.5 wt%, respectively, within 600 seconds, which are higher than that of 2.4 wt% in the pure as-milled MgH_2. When the temperatures are increased to 320 ˚C and 350 ˚C, the as-milled MgH_2-ANi_5 composites can still denote the better dehydrogenation kinetics than the pure ball-milled MgH_2 which only possesses the higher final desorption hydrogen capacities in a longer time.

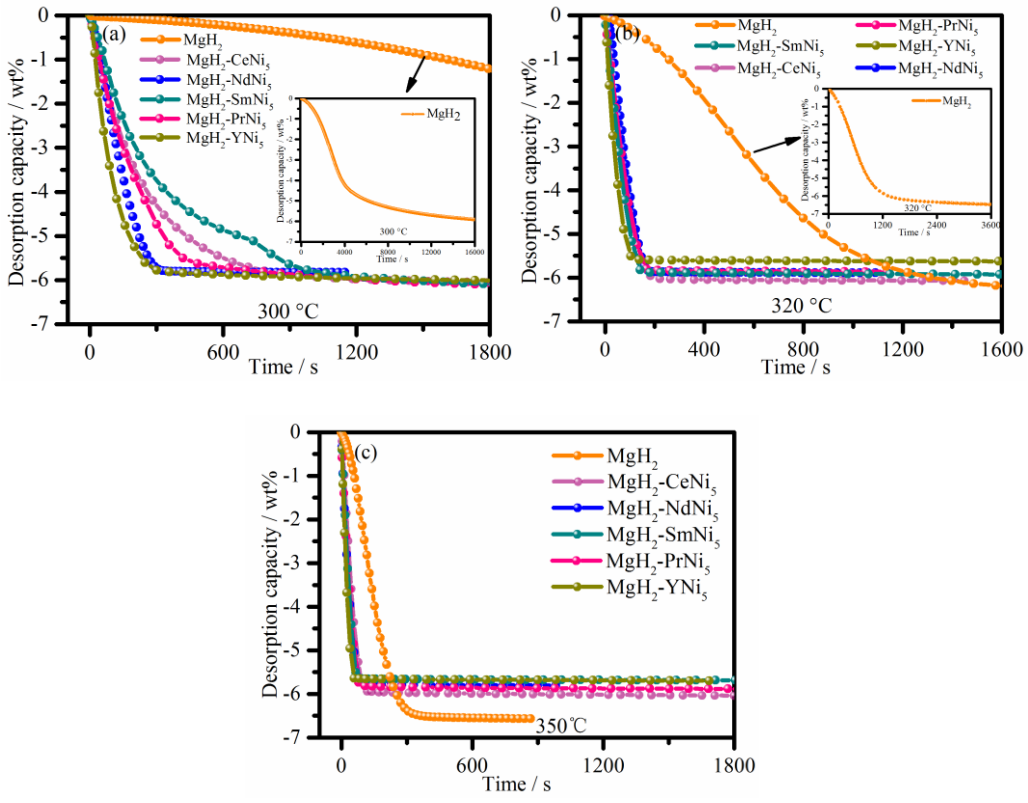

Fig. 7. The kinetic curves of hydrogen desorption of MgH_2-ANi_5 composites at different temperatures of (a) 300 ˚C, (b) 320 ˚C and (c) 350 ˚C respectively.

The decline in the final desorption capacity with increasing temperature in as-milled MgH_2-ANi_5 composites might be attributed to the rapid growth of grains at higher temperatures which give rise to the

decrease of hydrogen capacity and sluggish diffusivity of hydrogen in hydrides. It has been well known that the hydrogenation process of MgH_2 is dominated by the following three critical steps: 1) H_2 molecules decomposing into H atoms on the surface of the alloy, 2) H atoms diffusing along grain boundaries, and 3) hydrogenation of Mg atoms for transforming into MgH_2 molecules.[30] It is convinced that the decomposing energy of H_2 molecules into H atoms dominates the hydriding rate of Mg and it is fairly high in Mg/MgH_2 system.[43] In the present work, the Mg_2NiH_4 embedded on the surface of the matrix and the stable RE hydrides existed in the MgH_2-ANi_5 is incorporated to serve as hydrogen pumps, which may make it easier for hydrogen atoms to move through the metal matrix, thereby obviously speeding up the reaction rate of hydrogen absorption and desorption, as shown in Fig. 6-7.

Table 2

Summary of phase and hydrogen storage capacity about different ball milling samples.

Composite	Main phase after ball-milling	H_2 absorption capacity (wt%) at 2.5MPa			H_2 desorption capacity (wt%) at 0.1 MPa		
		300 ˚C	320 ˚C	350 ˚C	300 ˚C	320 ˚C	350 ˚C
MgH_2	MgH_2	6.41	6.75	6.65	5.82	6.47	6.58
MgH_2+$CeNi_5$	MgH_2; Mg_2NiH_4; CeH_3	6.09	5.98	6.21	6.16	6.08	6.05
MgH_2+$NdNi_5$	MgH_2; Mg_2NiH_4; NdH_3	6.07	5.80	6.22	5.71	5.92	5.80
MgH_2+$SmNi_5$	MgH_2; Mg_2NiH_4; SmH_3	6.10	6.20	6.02	6.38	5.96	5.72
MgH_2+YNi_5	MgH_2; Mg_2NiH_4; YH_3	5.92	5.80	5.78	6.50	5.64	5.70
MgH_2+$PrNi_5$	MgH_2; Mg_2NiH_4; PrH_3	6.26	5.97	6.21	6.21	5.85	5.90

Furthermore, as-milled MgH_2-$CeNi_5$ composite with different weight fractions of MgH_2 was chosen as an example to dissect the catalytic effect of ANi_5 alloy on the kinetic properties of Mg/MgH_2 system. Fig. 8 (a) and (b) give the dehydrogenation kinetic curves of MgH_2-$CeNi_5$ composite with various MgH_2 weight fraction (90 wt%, 95 wt% and 98 wt%) tested at temperatures of 300 ˚C and 320 ˚C, respectively. As for the dehydrogenation curves at the temperature of 300 ˚C shown in Fig. 8(a), it can be obtained that the

desorption hydrogen capacity of the as-milled MgH_2-$CeNi_5$ composite increases from 5.58 wt% to 6.16 wt% in 15 min with the weight fraction of MgH_2 increasing from 90 wt% to 95 wt%, while it decreases to 5.97 wt% in 30 min once the weight fraction of MgH_2 continually increases to 98 wt%. When the temperature goes up to 320 ˚C, however, the desorption hydrogen capacity of the as-milled MgH_2-$CeNi_5$ composite in Fig. 8(b) keeps increases from 5.8 wt%, 6.1 wt% to 6.4 wt% in 10min when the weight fraction of MgH_2 increases from 90 wt%, 95 wt% to 98 wt%, respectively. This might be due to that the lower temperature is more beneficial to activate the catalysis effects for improving the desorption kinetics.

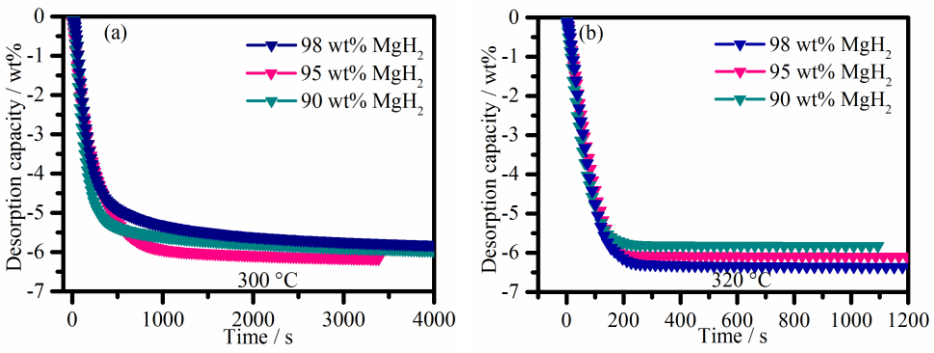

Fig. 8. The dehydrogenation kinetics curves of MgH_2-$CeNi_5$ composite with various MgH_2 weight fraction (90 wt%, 95 wt% and 98 wt%) tested at temperatures of (a) 300 ˚C and (b) 320 ˚C.

Finally, as-milled MgH_2− YNi_5 composite was chosen as representative to inspect the effect of ANi_5 alloys on the de/hydrogenation thermodynamic properties of the Mg/MgH_2 system. Fig. 9 gives the P.C.I. curves of MgH_2−YNi_5 composite at various temperatures of 280 ˚C, 300 ˚C and 320 ˚C, respectively. Seen from each PCI curve, there only contains one flat hydrogen platform demonstrating that only one phase participates in the hydrogenation process, which is consistent with the DSC curve. Obviously, the fairly flat absorption and desorption pressure plateaus correspond to the formation and dissociation of MgH_2. Based on the plateaus of pressure in Fig. 9, thermodynamics parameters, enthalpy ΔH and entropy ΔS can be derived from the van't Hoff equation as follow[44]

$$\ln\left(\frac{P_{H_2}}{P_0}\right) = \frac{\Delta H}{RT} - \frac{\Delta S}{R} \quad (4)$$

where P_0 is 1.01325×10^5 Pa, R is the mole gas constant, and P_{H_2} is the equilibrium plateau pressure corresponding to MgH_2. The enthalpy change ΔH and entropy change ΔS can be easily obtained respectively from the slopes and intercepts of the linearly fitting, as summarized in Fig. 9. According to Figure. 9, It's worth noting that the dehydriding reaction enthalpy is 78.23 kJ/mol and hydriding reaction enthalpy is -81.77 kJ/mol which are a little bit larger than the enthalpy 75 kJ/mol mentioned in the introduction. The increase in enthalpy of this alloy is due to the mixing of rare earth hydrides which have higher stability and higher enthalpy than MgH_2, this effect is also called the "Cocktail" effect.[45] The same phenomenon can be observed in many other similar systems, for example, the $Mg_{90}Ce_5Y_5$ system,[46] the $Mg_{88}Y_{12}$ system [47] and the Mg-Nd/Gd composite.[48]

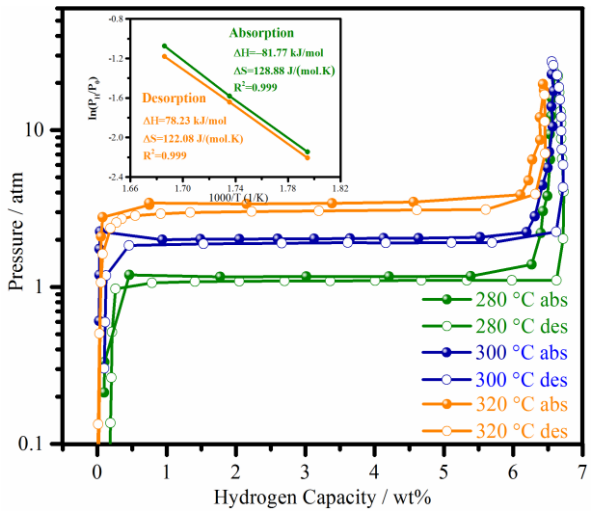

Fig. 9. P.C.I. curves and Van't Hoff plots of as-milled MgH_2-YNi_5 composite at temperatures of 280 ˚C, 300 ˚C and 320 ˚C respectively.

4. Conclusions

In summary, five MgH_2-ANi_5 (A = Ce, Nd, Pr, Sm, and Y) composites have been synthesized by mechanical ball milling to enhance the hydrogen storage properties of Mg/MgH_2 system, especially the

de/hydrogenation kinetic properties. The dehydrogenation temperature has been reduced from 423.4 ˚C in the pure MgH_2 without any additive to 288.8 ˚C, 284.2 ˚C, 287.6 ˚C, 287.3 ˚C and 287.3 ˚C respectively, in the as-milled MgH_2-ANi_5 (A = Ce, Nd, Pr, Sm, and Y) composites. Particularly, as-milled MgH_2-ANi_5 (A = Ce, Nd, Pr, Sm, and Y) composites can completely dehydrogenate within 600 s at the temperature of 300 ˚C, which exhibits excellent dehydrogenation kinetic performance. Besides, it is found that ANi_5 (A = Ce, Nd, Pr, Sm, and Y) could lead to a better catalytic effect on the desorption performance even at relatively lower temperatures of 300 ˚C. When changing the weight fraction of the MgH_2, it is revealed that MgH_2-$CeNi_5$ composite with 95 wt% MgH_2 can contribute to the highest desorption hydrogen capacity of 6.16 wt% in 15 min. Our results provide a guideline or strategy in the enhancement of light metal-based hydrogen storage materials by adding transition metallic catalysts.

Acknowledgements

This work was financially supported by the National Key R&D Program of China (No. 2018YFB1502101 and 2019YFB1505101), the Foundation for Innovative Research Groups of the National Natural Science Foundation of China (No. NSFC51621001), National Natural Science Foundation of China Projects (Nos. 51771075 and 51701171) and by the Project Supported by Natural Science Foundation of Guangdong Province of China (2016A030312011).

Reference

[1] Yu X, Tang Z, Sun D, Ouyang LZ, Zhu M. Recent advances and remaining challenges of nanostructured materials for hydrogen storage applications. Prog Mater Sci. 2017; 88: 1.

[2] Murthy S S, Kumar E A. Advanced materials for solid state hydrogen storage: “Thermal engineering issues”. Appl Therm Eng. 2014; 72(2): 176.

[3] Liu Y, Yang Y, Gao M, Pan H. Tailoring thermodynamics and kinetics for hydrogen storage in complex hydrides towards applications. Chem Rec. 2016; 16(1): 189.

[4] He T, Pachfule P, Wu H, Xu Q, Chen P. Hydrogen carriers. Nat Rev Mater. 2016; 1(12): 1.

[5] Zhu M, Lu Y, Ouyang LZ, Wang H. Thermodynamic tuning of Mg-based hydrogen storage alloys: a review. Materials. 2013; 6(10): 4654.

[6] Crivello JC, Dam B, Denys R, Dornheim M, Grant D, Huot J, et al. Review of magnesium hydride-based materials: development and optimisation. Appl Phys A Mater Sci Process. 2016; 122(2): 97.

[7] Jain I, Lal C, Jain A. Hydrogen storage in Mg: a most promising material. Int J Hydrogen Energy. 2010; 35(10): 5133.

[8] Nielsen TK, Manickam K, Hirscher M, Besenbacher F, Jensen T R. Confinement of MgH_2 nanoclusters within nanoporous aerogel scaffold materials. ACS nano. 2009; 3(11): 3521.

[9] Fu H, Wu W, Dou Y, Liu B, Li H, Peng Q. Hydrogen diffusion kinetics and structural integrity of superhigh pressure Mg-5 wt% Ni alloys with dendrite interface. J Power Sources. 2016; 320: 212.

[10] Zhang J, Yan S, Qu H. Recent progress in magnesium hydride modified through catalysis and nanoconfinement. Int J Hydrogen Energy. 2018; 43(3): 1545.

[11] Mustafa N, Ismail M. Hydrogen sorption improvement of MgH_2 catalyzed by CeO_2 nanopowder. J Alloys Compd. 2017; 695: 2532.

[12] Anastasopol A, Pfeiffer TV, Middelkoop J, Lafont U, Canales-Perez R J, Schmidt-Ott A, et al. Reduced enthalpy of metal hydride formation for Mg–Ti nanocomposites produced by spark discharge generation. J Am Chem Soc. 2013; 135(21): 7891.

[13] Lu Y, Wang H, Liu J, Ouyang LZ, Zhu M. Destabilizing the dehydriding thermodynamics of MgH_2 by reversible intermetallics formation in Mg−Ag−Zn ternary alloys. J Power Sources. 2018; 396: 796.

[14] Ouyang LZ, Cao Z, Wang H, Liu J, Sun D, Zhang Q, et al. Dual-tuning effect of in on the thermodynamic and kinetic properties of Mg_2Ni dehydrogenation. Int J Hydrogen Energy. 2013; 38(21): 8881.

[15] Yin Y, Li B, Yuan Z, Qi Y, Zhang Y. Enhanced hydrogen storage performance of Mg-Cu-Ni system catalyzed by CeO_2 additive. J of Rare Earths. 2019.

[16] Hanada N, Ichikawa T, Fujii H. Catalytic effect of nanoparticle 3d-transition metals on hydrogen storage properties in magnesium hydride MgH_2 prepared by mechanical milling. J Phys Chem B. 2005; 109(15): 7188.

[17] Patelli N, Calizzi M, Migliori A, Morandi V, Pasquini L. Hydrogen desorption below 150 ˚C in MgH_2–TiH_2 composite nanoparticles: equilibrium and kinetic properties. J Phys Chem C. 2017; 121(21): 11166.

[18] Jangir M, Jain A, Agarwal S, Zhang T, Kumar S, Selvaraj S, et al. The enhanced de/re‐hydrogenation performance of MgH_2 with TiH_2 additive. Int J Energy Res. 2018; 42(3): 1139.

[19] Sulaiman N, Mustafa N, Ismail M. Effect of Na_3FeF_6 catalyst on the hydrogen storage properties of MgH_2. Dalton Trans. 2016; 45(16): 7085.

[20] Malka I, Pisarek M, Czujko T, Bystrzycki J. A study of the ZrF_4, NbF_5, TaF_5, and $TiCl_3$ influences on the MgH_2 sorption properties. Int J Hydrogen Energy. 2011; 36(20): 12909.

[21] Idris N, Mustafa N, Ismail M. $MnFe_2O_4$ nanopowder synthesised via a simple hydrothermal method for promoting hydrogen sorption from MgH_2. Int J Hydrogen Energy. 2017; 42(33): 21114.

[22] Yahya M, Ismail M. Synergistic catalytic effect of $SrTiO_3$ and Ni on the hydrogen storage properties of MgH_2. Int J Hydrogen Energy. 2018; 43(12): 6244.

[23] Soni PK, Bhatnagar A, Shaz M, Srivastava O. Effect of graphene templated fluorides of Ce and La on

the de/rehydrogenation behavior of MgH_2. Int J Hydrogen Energy. 2017; 42(31): 20026.

[24] Sulaiman N, Juahir N, Mustafa N, Yap FH, Ismail M. Improved hydrogen storage properties of MgH_2 catalyzed with K_2NiF_6. J Energy Chem. 2016; 25(5): 832.

[25] Jalil Z. The role of SiC on the desorption temperature of Mg-based hydrogen storage materials prepared by intensive milling method. KnE Engineering. 2016.

[26] Bobet J, Akiba E, Nakamura Y, Darriet B. Study of Mg-M (M = Co, Ni and Fe) mixture elaborated by reactive mechanical alloying—Hydrogen sorption properties. Int J Hydrogen Energy. 2000; 25(10): 987.

[27] Ares J, Cuevas F, Percheron-Guégan A. Mechanical milling and subsequent annealing effects on the microstructural and hydrogenation properties of multisubstituted $LaNi_5$ alloy. Acta Mater. 2005; 53(7): 2157.

[28] Manchester FD. Phase diagrams of binary hydrogen alloys. ASM International, Member/Customer Service Center, Materials Park, OH 44073-0002, USA, 2000. 322. 2000.

[29] Liang G, Huot J, Boily S, Van Neste A, Schulz R. Hydrogen storage in mechanically milled Mg–$LaNi_5$ and MgH_2–$LaNi_5$ composites. J Alloys Compd. 2000; 297(1-2): 261.

[30] Rizo-Acosta P, Cuevas F, Latroche M. Hydrides of early transition metals as catalysts and grain growth inhibitors for enhanced reversible hydrogen storage in nanostructured magnesium. J Mater Chem A Mater. 2019; 7(40): 23064.

[31] Ouyang LZ, Yang X, Zhu M, Liu J, Dong H, Sun D, et al. Enhanced hydrogen storage kinetics and stability by synergistic effects of in situ formed $CeH_{2.73}$ and Ni in $CeH_{2.73}$-MgH_2-Ni nanocomposites. J Phys Chem C. 2014; 118(15): 7808.

[32] Xie L, Li J, Zhang T, Song L. Dehydrogenation steps and factors controlling desorption kinetics of a MgCe hydrogen storage alloy. Int J Hydrogen Energy. 2017; 42(33): 21121.

[33] Yong H, Guo S, Yuan Z, Qi Y, Zhao D, Zhang Y. Improved hydrogen storage kinetics and thermodynamics of RE-Mg-based alloy by co-doping Ce–Y. Int J Hydrogen Energy. 2019; 44(31): 16765.

[34] Zhang Q, Zang L, Huang Y, Gao P, Jiao L, Yuan H, et al. Improved hydrogen storage properties of MgH_2 with Ni-based compounds. Int J Hydrogen Energy. 2017; 42(38): 24247.

[35] Delchev P, Himitliiska T, Spassov T. Microstructure and hydriding properties of ball-milled Mg–10 at.% $MmNi_5$ (Mm = La, Ce-rich mischmetal) composites. J Alloys Compd. 2006; 417(1-2): 85.

[36] Zhang Y, Dianchen F, Hao S, Wengang B, Yan Q, Shihai G. Structure and electrochemical hydrogen storage characteristics of Ce-Mg-Ni-based alloys synthesized by mechanical milling. J Rare Earths. 2017; 35(3): 280.

[37] Dong HW, Ouyang LZ, Sun T, Zhu M. Effect of ball milling on hydrogen storage of Mg_3La alloy. J Rare Earths. 2008; 26(2): 303.

[38] Huot J, Liang G, Boily S, Van Neste A, Schulz R. Structural study and hydrogen sorption kinetics of ball-milled magnesium hydride. J Alloys Compd. 1999; 293: 495.

[39] Zhang Q, Liu D, Wang Q, Fang F, Sun D, Ouyang LZ, et al. Superior hydrogen storage kinetics of $Mg_{12}YNi$ alloy with a long-period stacking ordered phase. Scr Mater. 2011; 65(3): 233.

[40] Wang J, Li Y, Liu T, Peng D, Han S. Synthesis of Mg-based composite material with in-situ formed LaH_3 and its hydrogen storage characteristics. J Rare Earths. 2018; 36(7): 739.

[41] Cui J, Liu J, Wang H, Ouyang LZ, Sun D, Zhu M, et al. Mg–TM (TM: Ti, Nb, V, Co, Mo or Ni) core–shell like nanostructures: synthesis, hydrogen storage performance and catalytic mechanism. J Mater Chem A Mater. 2014; 2(25): 9645.

[42] Zhang YH, Zhang W, Yuan ZM, Bu WG, Yan Q, Dong XP, et al. Hydrogen storage performances of as-milled $REMg_{11}Ni$ (RE = Y, Sm) alloys catalyzed by MoS_2. T Nonferr Metal Soc. 2018; 28(9): 1828.

[43] Sakintuna B, Lamari-Darkrim F, Hirscher M. Metal hydride materials for solid hydrogen storage: a review. Int J Hydrogen Energy. 2007; 32(9): 1121.

[44] Pourabdoli M, Raygan S, Abdizadeh H, Uner D. Determination of kinetic parameters and hydrogen desorption characteristics of MgH_2-10 wt%(9Ni–2Mg–Y) nano-composite. Int J Hydrogen Energy. 2013; 38(27): 11910.

[45] Ranganathan S. Alloyed pleasures: Multimetallic cocktails. Curr Sci. 2003; 85(10): 1404.

[46] Lin HJ, Ouyang LZ, Wang H, Zhao DQ, Wang WH, Sun DL, et al. Hydrogen storage properties of Mg-Ce-Ni nanocomposite induced from amorphous precursor with the highest Mg content. Int J Hydrogen Energy. 2012; 37(19): 14329.

[47] Yang T, Yuan Z, Bu W, Jia Z, Qi Y, Zhang Y. Evolution of the phase structure and hydrogen storage thermodynamics and kinetics of $Mg_{88}Y_{12}$ binary alloy. Int J Hydrogen Energy. 2016; 41(4): 2689.

[48] Zou J, Zeng X, Ying Y, Chen X, Guo H, Zhou S, et al. Study on the hydrogen storage properties of core-shell structured Mg-RE (RE = Nd, Gd, Er) nano-composites synthesized through arc plasma method. Int J Hydrogen Energy. 2013; 38(5): 2337.

TOC Graphic:

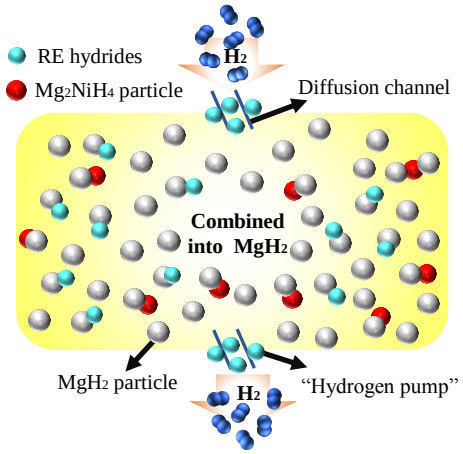

In-situ formed Mg_2Ni and stable RE hydride small particles are attached to the surface to form a diffusion channel together with the defect, and also serving as a hydrogen pump so that the kinetic properties of MgH_2 can be improved significantly.